LLNL-PROC-713180

LAWRENCE
LIVERMORE
NATIONAL
LABORATORY

Impacts of SiO2 planarization on optical thin film properties and laser damage resistance

T. Day, H. Wang, E. Jankowska, B. Reagan, J. Rocca, C. Menoni, C. Stolz, P. Mirkarimi, J. Folta, J. Roehling, A. Markosyan, R. Route, M. Fejer

December 6, 2016

SPIE Laser Damage
Boulder, CO, United States
September 25, 2016 through September 28, 2016

Impacts of SiO_2 planarization on optical thin film properties and laser damage resistance

T. Day*[1], H. Wang[1], E. Jankowska[1], B. Reagan[1], J. Rocca[1], C. Menoni[1], C. J. Stolz[2], P. Mirkarimi[2], J. Folta[2], J. Roehling[2], A. Markosyan[3], R. Route[3], M. Fejer[3]

[1]Department of Electrical and Computer Engineering, Colorado State University, Fort Collins, CO 80523, USA; [2]Lawrence Livermore National Laboratory, P.O. Box 808, L-460, Livermore, CA 94551 USA; [3]Department of Applied Physics, E.L. Ginzton Laboratory, Stanford University, Stanford, CA 94305, USA; *corresponding author: travis.day@colostate.edu

ABSTRACT

Lawrence Livermore National Laboratory (LLNL) and Colorado State University (CSU) have co-developed a planarization process to smooth nodular defects. This process consists of individually depositing then etching tens of nanometers of SiO_2 with a ratio of 2:1, respectively. Previous work shows incorporating the angular dependent ion surface etching and unidirectional deposition reduces substrate defect cross-sectional area by 90%. This work investigates the micro-structural and optical modifications of planarized SiO_2 films deposited by ion beam sputtering (IBS). It is shown the planarized SiO_2 thin films have approximately 3x increase in absorption and slight reduction in thin film stress as compared to control (as deposited) SiO_2. Planarized SiO_2 films exhibit little change in RMS surface roughness with respect to the control and super polished fused silica substrates. Laser induced damage threshold (LIDT) results indicate slight film modification changes with planarization processing where films damage at similar onset fluences yet have sharper damage curves.

Keywords: Planarization, nodular defects, ion beam sputtering, laser induced damage, silica

1. INTRODUCTION

From the advent of the laser, laser-induced damage (LID) of various optical components has been a limiting issue for the development of modern higher power laser systems. Often nodules are the lowest fluence limiting defects of multilayer interference coatings.[1-4] These defects, created from surface deformations, scratches, dust, improper substrate cleaning, impurities, or coating flakes, cause large deformations in the coating surface which in turn induces light intensification leading to catastrophic coating damage and nodule ejection.[1-7] To address this common issue, particularly with large aperture optics, LLNL and CSU have co-developed a planarization surface smoothing process.[8-11] Planarization processing through ion bombardment and etching was originally developed to smooth substrate particles for extreme ultraviolet (EUV) multilayer mirrors and lithography.[12-13] This deposition process has the capability to smooth over micron-size nodules at the substrate surface or within the multilayer coatings. When applied to engineered nodular defects, a 20x improvement in the LIDT has been observed with control engineered coatings.[8] Yet, when applied to real (non-engineered) coatings, the planarized mirrors have increased damage density per square centimeter raster scanned areas and damages with flat-bottomed interfacial damage craters with depths correlating to the top planarized SiO_2 layers.[14] These discoveries prompted a more extensive investigation of the SiO_2 planarized films.

In previous work, cylindrical nodular defects were engineered by contact lithography and ion etching and then planarized over with both thick SiO_2 layers at the substrate-coating surface or through planarizing SiO_2 layers within the multilayer mirror.[8-10] This work is specifically aimed at identifying the defects created, impurities implanted, linear absorption, thin film stress, surface roughness, and laser damage characteristics of planarized SiO_2 and HfO_2/SiO_2 bilayer films. Bilayer films, which emulate the optical interference coating multilayer structure, were investigated to extrapolate possible changes with SiO_2 planarization within multilayers.

2. EXPERIMENT

Planarization processing, discussed in depth elsewhere [10,11], involves multiple discrete grow and etch cycles, in a 2:1 ratio, to smooth nodular defects. Within multilayer interference coatings, 8 planarization cycles are repeated (deposition then etch) per λ /4 SiO_2 layer or until the desired thickness is reached.

The coatings were fabricated by dual ion beam sputtering (IBS) using a Veeco Spector® system and deposited upon super polished UV-grade fused silica substrates (.5-mm-thick substrates were used in measuring the stress, otherwise .25-inch-thick substrates were used). A set of 350 nm (λ/2 at 1030 nm) as deposited and planarized SiO_2 films were fabricated and 125 nm (λ/4 at 1030 nm) HfO_2 films were then deposited upon a second set of these SiO_2 coatings. The SiO_2 film were sputtered from an oxide target and HfO_2 films from a metallic target and the conditions of deposition and etching was 1.25 keV and 600 mA and 1 keV and 150 mA, respectively.

The SiO_2 is etched with 1 keV argon (Ar) ions accelerated through molybdenum (Mo) grids. These ions or grid material have the potential to implant into the film and alter the optical, micro-structural properties, or laser damage morphology. A diagram of the planarization process with discreet deposit and etch cycles is shown in Figure 1. Thin red bands represent the approximately 3 nm penetration depth of 1 keV Ar ions calculated from SRIM Monte Carlo modeling. The short penetration depth leads to small bands throughout the thickness of the coating where Ar implantation, Mo contamination, or other defects may lie.

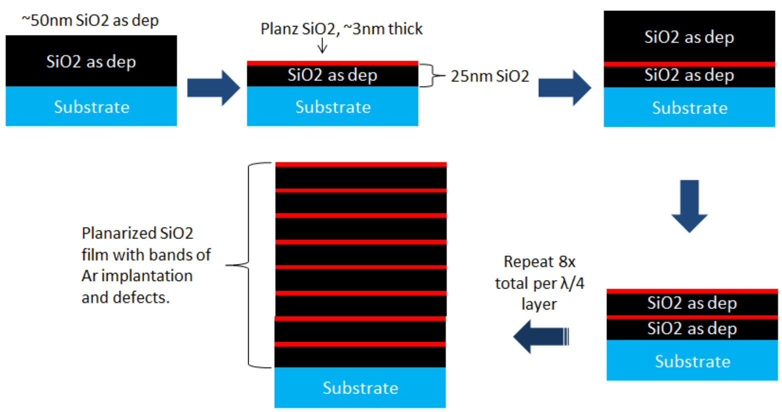

Figure 1: This diagram shows the steps involved in the planarization (planz) process. The red thin bands represent approximately 3 nm penetration depth of Ar ions.

The surface roughness was characterized with a Zygo Scanning White Light Interferometer (SWLI) which measured the roughness at 5 unique and random locations throughout the film surface with 100x microscope objective and 0.11nm axial resolution.

The amorphous films were deposited on a .5 mm thick substrate was measured by a Twyman-Green interferometer employing carrier frequency interferometry to extract the film radius of curvature.[15] Stoney's formula was then used to find the thin film stress.

Photothermal common-path interferometry (PCI) [16] employing a 1064 nm Nd:YAG fiber amplified pump and 632.8 nm HeNe probe laser was used to measure the absorption loss of the coatings in parts per million (ppm). Each sample was measured at 5 unique locations and the values averaged.

X-ray photoelectron spectroscopy (XPS) and energy-dispersive X-ray spectroscopy (SEM-EDS) were used to investigate implanted impurities originating from the ion source grids (Mo) or ions themselves (Ar). A high-resolution PE-5800 XPS instrument with Cu K_α radiation and a JEOL JSM-6500F SEM equipped with an electron energy dispersive X-ray spectrometer (EDS) were used.

The LIDT characteristics are a critical feature in many optical components for high fluence applications. For the scope of this work, 1-on-1 and 500-on-1 LIDT measurements were carried out with a 100 μm (e^{-2}) spot size and corresponding to ISO: 21254. The damaging laser was a 1030nm Yb:YAG mode-locked oscillator with a regenerative amplifier operating at 220 ps and, a fiber diode pumped, cryogenically cooled 2nd amplifying stage with 70 mJ output at 20 Hz. [17] Coating damage was detected with an *in situ* scatter microscope and *ex situ* Nomarski microscope at 40x and 100x. Below, Figure 2 displays the optical setup for LIDT testing.

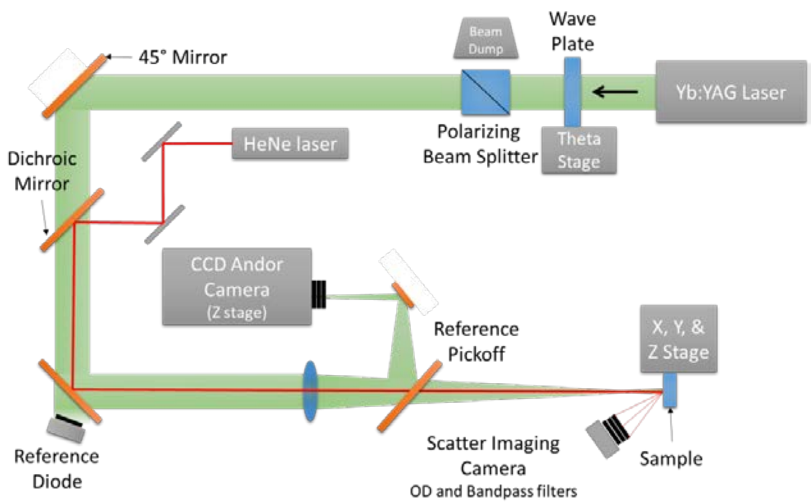

Figure 2: Schematic diagram of laser damage setup.

3. RESULTS

Table 1: A summary of the coating samples tested, thickness, surface roughness, thin film stress, and absorption loss. The uncertainties reported are calculated using corrected sample standard deviation.

Sample	**Thickness (nm)**	**RMS Surface Roughness (Å)**	**Film Stress (MPa)**	**PCI Absorption Loss (ppm)**
UV grade Fused Silica	N/A	2.8 ± 0.5 Å	N/A	28.1 ppm/cm
SiO_2 as dep	350 nm	2.9 ± 0.6 Å	δ = 275 MPa	5.70 ± 0.08 ppm
SiO_2 planarized	350 nm	3.3 ± 0.1 Å	δ = 231 MPa	17.2 ± 0.2 ppm
HfO_2/ SiO_2 as dep	125 nm / 350 nm	N/A	δ = 225 MPa	8.0 ± 0.2 ppm
HfO_2/ SiO_2 planarized	125 nm / 350 nm	N/A	δ = 212 MPa	18.5 ± 0.3 ppm
HfO_2 single	125 nm	N/A	N/A	5.1 ± 0.1 ppm

Table 1 summarizes the thin film samples tested and their respective thickness, surface roughness, thin film stress, and absorption loss. It was found the RMS surface roughness is slightly increased by ~13% from as deposited SiO_2 and ~16% from the polished substrate. Yet, the roughness is still well within acceptable parameters for optical performance. Incidentally, planarization is optimized to smooth large, micron-sized contaminates and nodules yet, has little to no effect one RMS roughness when utilized without these defects present. The SiO_2 planarized has approximately -18% change in the thin film stress as compared with the SiO_2 as deposited. While the HfO_2 capped SiO_2 films have over all less stress than the single SiO_2.

The SiO_2 planarized and HfO_2 capped SiO_2 planarized coatings have a 3x and 2.3x increase in absorption loss, respectively. This observation prompted further characterization techniques to uncover the cause of this absorption increase. These films were also annealed at 300°C for 8 hours in air at atmospheric pressure. An improvement in the absorption loss of the coatings is shown in Figure 3. High energy (10's keV) ion implantation has been observed to create various oxygen deficiency point defects and annealing was shown to recover these defects.[18,19] Additional photothermal microscopy has been used to observe nano-absorption LID precursors.[20] It is likely that these nano-absorber defects are playing a major role in the film absorption.

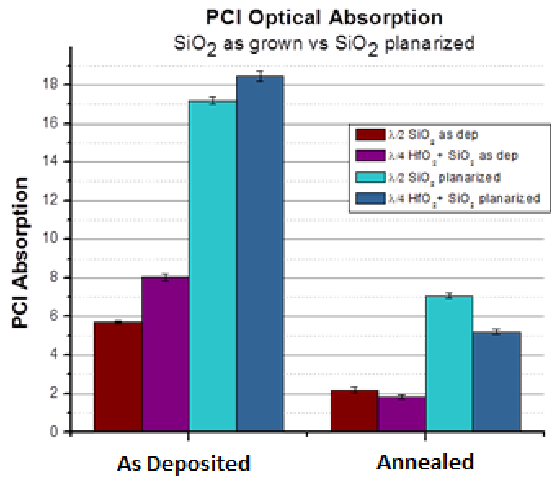

Figure 3: Bar graph comparing PCI absorption (ppm) of SiO_2 as deposited, SiO_2 planarized and HfO_2 capped SiO_2 films. Right shows the absorption loss decreases after annealing at 300°C for 8 hours.

.

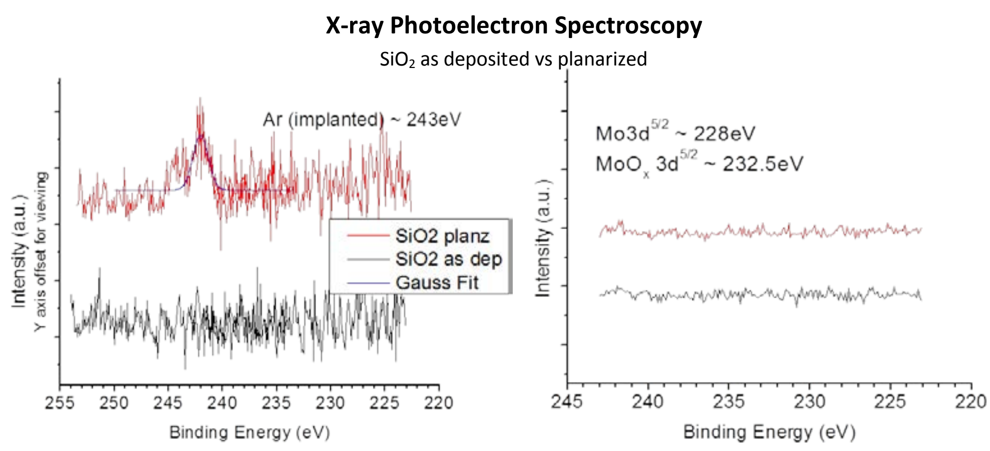

Figure 4: XPS data comparing SiO_2 as deposited vs planarized.

With XPS there were no peaks found at the 3d5/2 photoelectron of metallic Mo in both SiO_2 films and a small amount of implanted Ar, at the 2p1/2 photoelectron line, was found within the planarized SiO_2 film only. As Figure 4 shows, there is less Mo than the minimum detectable limit of the XPS, of about part per thousand. The SEM-EDS, a slightly more sensitive technique, may provide added information about the coating impurities. Full elemental EDS scans and high resolution scans around the known lines of Mo and Ar were carried out and shown in Figure 5.

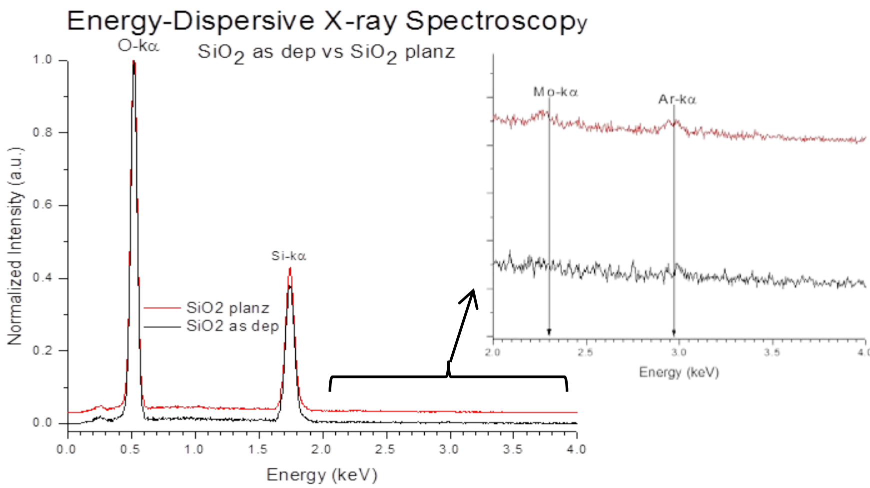

Figure 5: SEM-EDS comparing SiO_2 as deposited vs planarized.

Even with adequately long counting times the Mo L_α and Ar k_α lines at 2.293 keV and 2.957 keV, respectively, peaks have very little form and scarcely rise above the continuum background noise. It is believed that there are insignificant amounts of contamination detected to be a considerable factor in the increased absorption or laser damage morphology.

The 1-on-1 LIDT results, Figure 6, showed similar onset fluences for all films of about 11-13 J/cm^2, yet both SiO_2 planarized coatings have sharper damage probability curves. For laser damage resistance, HfO_2 is often claimed to be the limiting material in multilayer coatings,[21] however it is not the case here. A 20-40% decrease in the 50% and 100% damage probabilities of planarized SiO_2 and HfO_2 capped planarized SiO_2 was observed. For comparison, the UV grade fused silica substrate was also LIDT tested and has an onset fluence of about 33 J/cm^2. The sharp LID probability curves signify a greater density of nano-absorber defects throughout the entire film.

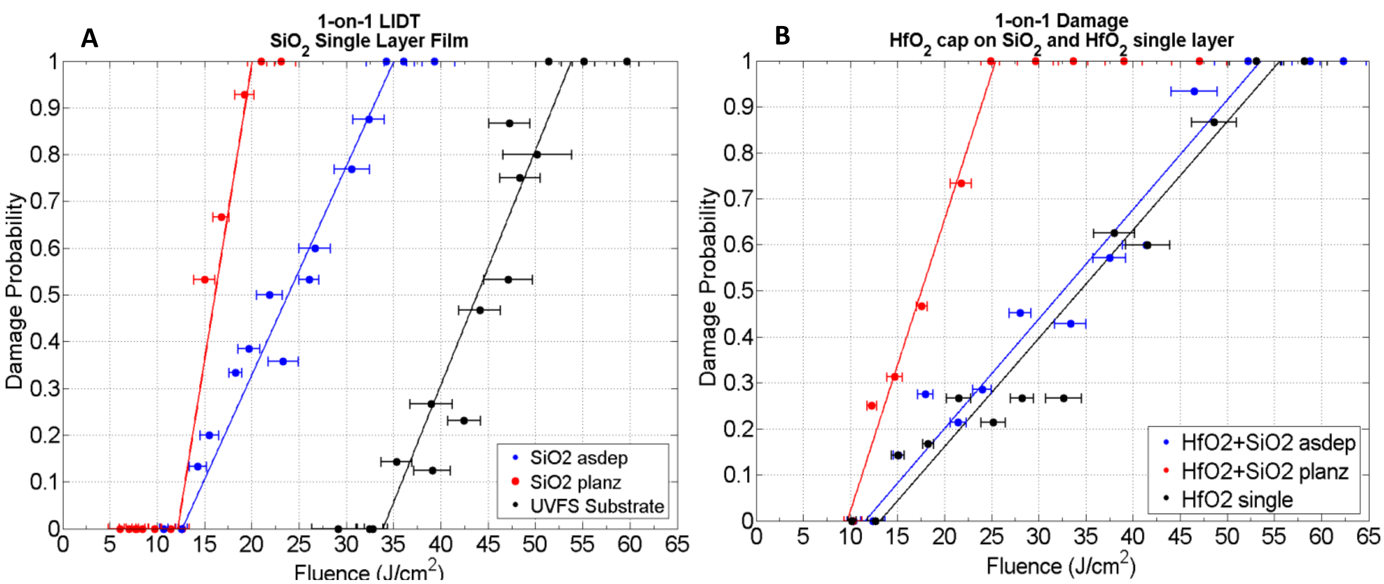

Figure 6: LIDT probability data showing 1-on-1 damage at 1030nm and 220ps of (A) SiO_2 single layers (as deposited and planarized) and UV grade fused silica substrate and (B) HfO_2 capped SiO_2 films and HfO_2 single layers. Error bars correspond to the standard deviation error calculated from variations in pulse energy and spot size.

The damage morphology, Figure 7, shows damage pitting as small as ~3 μm in diameter at damage onset fluences. These pits accumulate at higher fluences. In most cases, the planarized SiO_2 coatings have larger density of damage pits in the irradiated area, at the same damage probability fluence. HfO_2 capped SiO_2 exhibited in a similar damage morphology trend. This damage morphology has been previously linked to nano-absorption induced LID initiation.[22-24] Further, this damage morphology was seen by L. Gallais et al. in HfO_2 single layers and effectively modeled by metallic Hf and non-stoichiometric HfO_2 inclusions.[22]

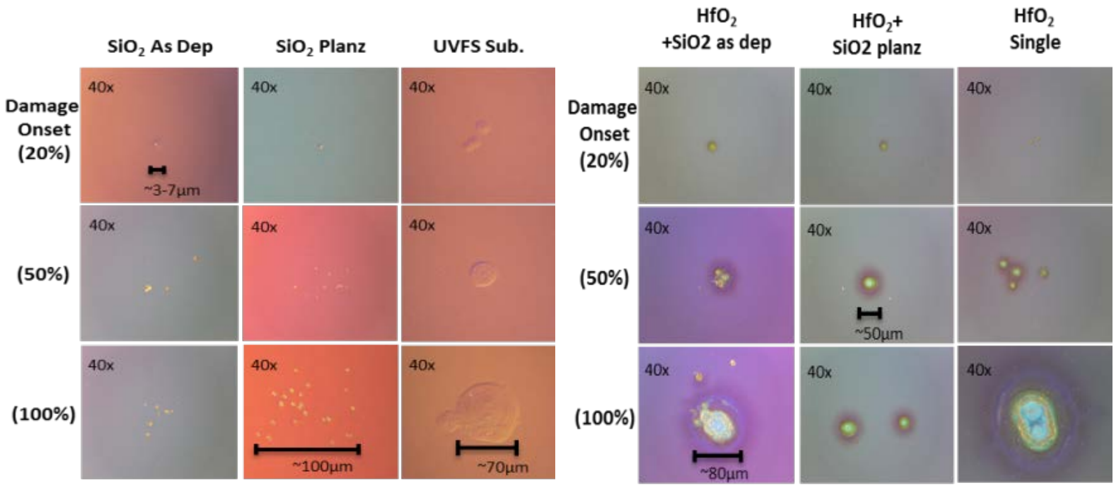

Figure 7: Nomarski images characteristic damage craters at damage onset, 50% damage, and 100% damage for SiO_2 films and HfO_2 capped SiO_2 films.

To investigate the LID growth of these samples, 500-on-1 LIDT measurements were completed. Figure 8A displays the damage probability curve with and without growth and damage craters. It was observed, in Figure 8B, that low fluence damage does not grow with successive pulses. The damage growth region begins around 30–35 J/cm^2 and produces approximately 400 μm damage craters which penetrate the substrate. Additionally, the diameter of these craters and density of pits within the irradiated area increase with higher fluences. Within the non-growth region, planarized SiO_2 again damaged with a higher density of damage pitting. As discussed above, this damage pitting is likely linked to nano-absorber initiation sites consisting of metallic bonds or oxygen deficiency defects.

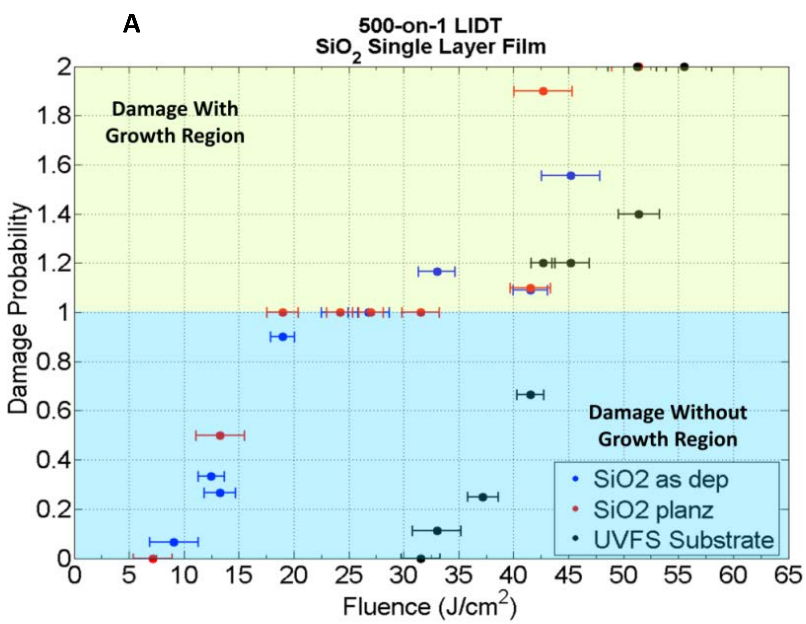

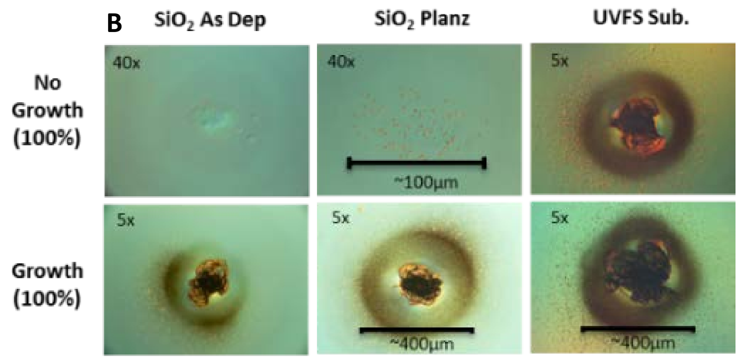

Figure 8: (A) LIDT probability data showing 500-on-1 damage of SiO_2 single layers (as deposition and planarized) and UV grade fused silica substrate. The region between 0 and 1 damage probability indicates damage which does not grow whereas the region between 1 and 2 damage probability indicates damage which grows with successive pulses. (B) Nomarski images characteristic damage craters at 100% damage without growth and 100% damage with growth for SiO_2 films.

4. CONCLUSION

In this work, the optical, micro-structural properties, and laser damage resistance of IBS SiO_2 as grown and planarized have been investigated. It was found the absorption loss of planarized SiO_2 films is about 3x that of the control samples and post-annealing decreases these losses. Insignificant amounts of Mo and Ar contamination was found and a slight reduction in the stress was observed. LIDT measurements show both SiO_2 and HfO_2 coatings damage at similar fluences, yet planarized SiO_2 coatings have sharper damage probability curves. The sharp LID probability curves, increased damage pitting morphology, and increased absorption which decreases after annealing indicate metallic bonds or oxygen deficiency nano-absorption sites as probable candidates for damage in planarized SiO_2 films. This can limit the LID when nodular defects are not present. Annealing was shown to reduce the absorption loss of the coatings and should be further investigated in relation to defect recovery and LID behavior.

Overall, planarization processing is effective in mitigating low fluence nodular defects in optical interference coatings and does not significantly affect the microstructure, optical properties, or LIDT when tested at 1030 nm wavelength and 220 ps pulse duration.

5. ACKNOWLEDGEMENTS

This work was performed under the auspices of the U.S. Department of Energy by Lawrence Livermore National Laboratory under Contract DE-AC52-07NA27344.

6. REFERENCES

1. Guenther, Karl H. "Nodular defects in dielectric multilayers and thick single layers." *Applied optics* 20.6 (1981): 1034-1038.
2. Stolz, Christopher J., et al. "Comparison of nodular defect seed geometries from different deposition techniques." *Laser-Induced Damage in Optical Materials: 1995*. International Society for Optics and Photonics, 1996.
3. Cheng, Xinbin, et al. "Laser damage study of nodules in electron-beam-evaporated HfO 2/SiO 2 high reflectors." *Applied optics* 50.9 (2011): C357-C363.
4. Cheng, Xinbin, et al. "Nanosecond laser-induced damage of nodular defects in dielectric multilayer mirrors [Invited]." *Applied optics* 53.4 (2014): A62-A69.
5. Cheng, Xinbin, et al. "The effect of an electric field on the thermomechanical damage of nodular defects in dielectric multilayer coatings irradiated by nanosecond laser pulses." *Light: Science & Applications* 2.6 (2013): e80.
6. Cheng, Xinbin, et al. "Physical insight toward electric field enhancement at nodular defects in optical coatings." *Optics express* 23.7 (2015): 8609-8619.

7. Qiu, S. Roger, et al. "Impact of substrate surface scratches on the laser damage resistance of multilayer coatings." *Laser Damage Symposium XLII: Annual Symposium on Optical Materials for High Power Lasers*. International Society for Optics and Photonics, 2010.
8. Stolz, Christopher J., et al. "Defect insensitive 100 J/cm2 multilayer mirror coating process." *SPIE Laser Damage*. International Society for Optics and Photonics, 2013.
9. Stolz, Christopher J., et al. "High laser-resistant multilayer mirrors by nodular defect planarization [Invited]." *Applied optics* 53.4 (2014): A291-A296.
10. Stolz, Christopher J., et al. "Substrate and coating defect planarization strategies for high-laser-fluence multilayer mirrors." *Thin Solid Films* 592 (2015): 216-220.
11. C. J. Stolz, J. A. Folta, P. B. Mirkarimi, R. Soufli, C. C. Walton, J. E. Wolfe, C. S. Menoni, D. Patel, "Planarization of multilayer optical coating defects," Provisional Patent Attorney Docket Number IL-12580 (2012).
12. Mirkarimi, P. B., et al. "A silicon-based, sequential coat-and-etch process to fabricate nearly perfect substrate surfaces." *Journal of nanoscience and nanotechnology* 6.1 (2006): 28-35.
13. Mirkarimi, P. B., et al. "Advancing the ion beam thin film planarization process for the smoothing of substrate particles." *Microelectronic engineering* 77.3 (2005): 369-381.
14. Stolz, Christopher J., et al. "Depth determination of critical fluence-limiting defects within planarized and non-planarized mirror coatings." *SPIE Optical Systems Design*. International Society for Optics and Photonics, 2015.
15. Jankovska, Elzbieta, Slawomir Drobczynski, and Carmen S. Menoni. "Analysis of surface deformation by carrier frequency interferometry." *Optical Interference Coatings*. Optical Society of America, 2016.
16. Alexandrovski, Alexei, et al. "Photothermal common-path interferometry (PCI): new developments." *SPIE LASE: Lasers and Applications in Science and Engineering*. International Society for Optics and Photonics, 2009.
17. Baumgarten, Cory, et al. "1 J, 0.5 kHz repetition rate picosecond laser." *Optics Letters* 41.14 (2016): 3339-3342.
18. Devine, R. A. B., and A. Golanski. "Creation and annealing kinetics of magnetic oxygen vacancy centers in SiO2." *Journal of Applied Physics* 54.7 (1983): 3833-3838.
19. Devine, R. A. B. "Oxygen vacancy creation in SiO2 through ionization energy deposition." *Applied physics letters* 43.11 (1983): 1056-1058.
20. Commandré, Mireille, J-Y. Natoli, and Laurent Gallais. "Photothermal microscopy for studying the role of nano-sized absorbing precursors in laser-induced damage of optical materials." *The European Physical Journal Special Topics* 153.1 (2008): 59-64.
21. Kaiser, Norbert, and Hans K. Pulker, eds. *Optical interference coatings*. Vol. 88. Springer, 2013.
22. Gallais, Laurent, et al. "Investigation of nanodefect properties in optical coatings by coupling measured and simulated laser damage statistics." *Journal of Applied Physics* 104.5 (2008): 053120.
23. Papernov, S., and A. W. Schmid. "Correlations between embedded single gold nanoparticles in SiO2 thin film and nanoscale crater formation induced by pulsed-laser radiation." *Journal of Applied Physics* 92.10 (2002): 5720-5728.
24. Batavičiutė, Gintarė, et al. "Revision of laser-induced damage threshold evaluation from damage probability data." *Review of Scientific Instruments*84.4 (2013): 045108.